



Effects of operating parameters on weld bead morphology with welding operations of API 5L X70 steel pipes by SMAW process

Hadjer Bensiali¹ · Lyes Bidi² · Eugen Cicala^{3,4} · Philippe Le Masson⁵ · Mohamed El Bahi Chibani⁶ · Mohamed Salah Boulahlib¹

Received: 12 September 2019 / Accepted: 27 January 2021 / Published online: 4 February 2021
© International Institute of Welding 2021

Abstract

The work presented in this paper deals with the study of the influence of the operating parameters of welding on observables which are the geometrical characteristics of the melted zone. In this study, the method implemented is of the SMAW (Shielded metal arc welding) manual arc type and is used to assemble the pipes through the filling of a V-shaped chamfer between two tubes 1219.5 mm in diameter, 13 mm thick, and a material of grade X70 steel. In order to increase the productivity and reliability of the chamfer filling operation, we used the experimental designs method, on the one hand to estimate the effects of the operating parameters and their interactions on several functions characterizing the morphology of the weld bead, and on the other hand, to provide a mathematical model that links the welding process operating parameters to the objective functions studied.

Keywords Pipe welding · SMAW process · Experimental designs · Weld bead morphology · Response surfaces

1 Introduction

World energy consumption is constantly increasing, always requiring new infrastructure, therefore the need for increasingly important welding technology, with an assurance of good quality weld beads and consequently a mastery of the welding processes and operating parameters. The development of pipelines

transport networks is the thematic that imposes itself today, because it is the best way to ensure the supply of energy for the industry and for the transportation of crude oil for export.

Considering the importance, in economic terms, of the development of the hydrocarbons pipelines transport sector for Algeria, SONATRACH transports crude oil, natural gas, LPG, and condensate, either towards the north of the country (to the refineries) or to the production complexes. It also has a pipeline network of 16.200 km which includes 12 gas pipelines (7.459 km) with a transport capacity of 131 billion m³/year. The pipeline transport activity in Algeria has 79 pumping and compression stations with 290 main machines, with a storage capacity of nearly 3.4 million m³, a port loading capacity of nearly 210 MTA, a maintenance, and servicing infrastructure on three main bases and three regional bases of intervention, a CNDG gas dispatching center (Hassi R'mel), and another CDHL liquid hydrocarbon dispatching center (Haoud El Hamra).

A pipeline is the assembly of several pipes by welding, requiring productive and low-cost welding processes, to ensure reliable weld beads. SMAW manual arc welding is the most widely used process in the oil industry, in view of these multiple benefits [1]. SMAW welding is performed in all positions [2], allows a great autonomy, and the required equipment is inexpensive. The heat transfer coefficient of the process (i.e., the amount of heat transmitted on a piece rate) varies between 50

✉ Lyes Bidi
lyes.bidi@umc.edu.dz

¹ Laboratoire Ingénierie des Transports et Environnement, Université Frères Mentouri Constantine 1, Constantine, Algeria

² Institut des Sciences et Techniques Appliquées, Université Frères Mentouri Constantine 1, Constantine, Algeria

³ Laboratoire Inter disciplinaire Carnot de Bourgogne, UMR 6303 CNRS, Dijon, France

⁴ Université de Bourgogne, IUT, 12 rue de la Fonderie, 71200 Le Creusot, France

⁵ Université. Bretagne Sud, FRE CNRS 3744, IRDL, F-56100 Lorient, France

⁶ SONATRACH, transport par canalisation, division exploitation, Région transport IN-AMENAS(RTI), Station de pompage LR1-RNS (Rhourde-Nouss), Algiers, Algeria

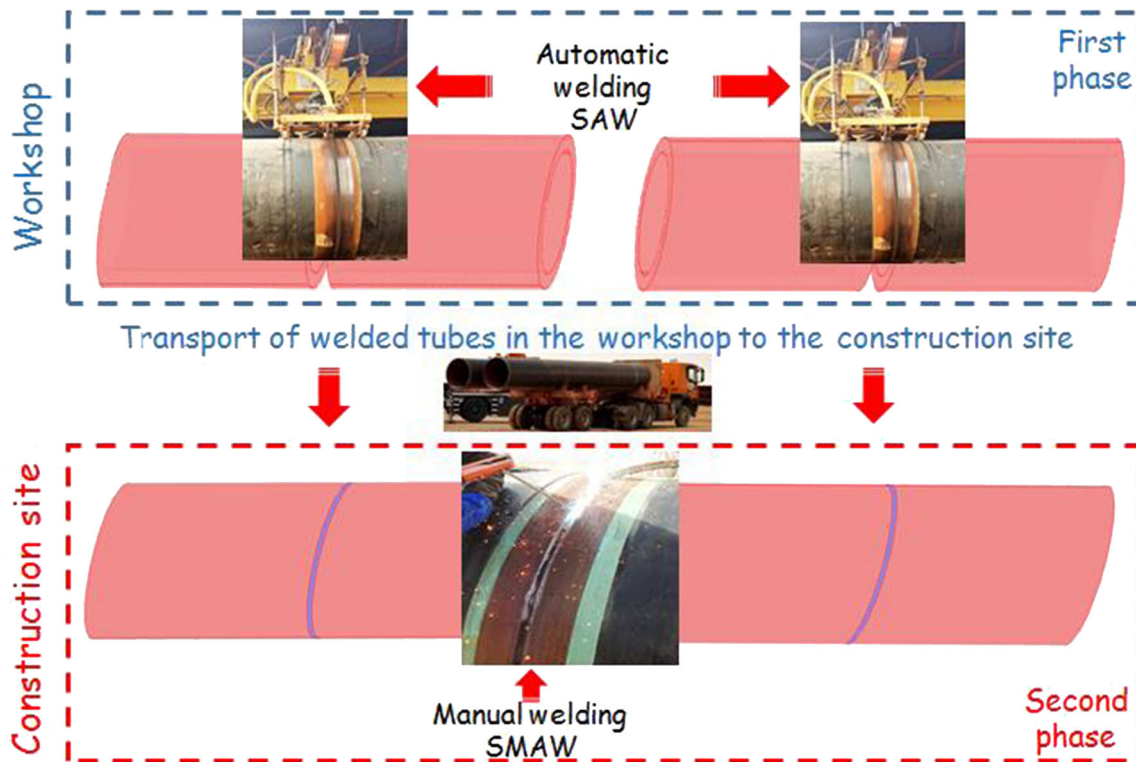


Fig. 1 Presentation of the different phases of pipeline assemblies

and 85%. As the penetration depth of the weld increases according to this coefficient, the SMAW can achieve good penetration. The arc's energy increases the quality of the finished

weld beads as well as the productivity. The SMAW process is more complex than the automatic SAW (submerged automatic welding) [3–8], because of the number of operating parameters

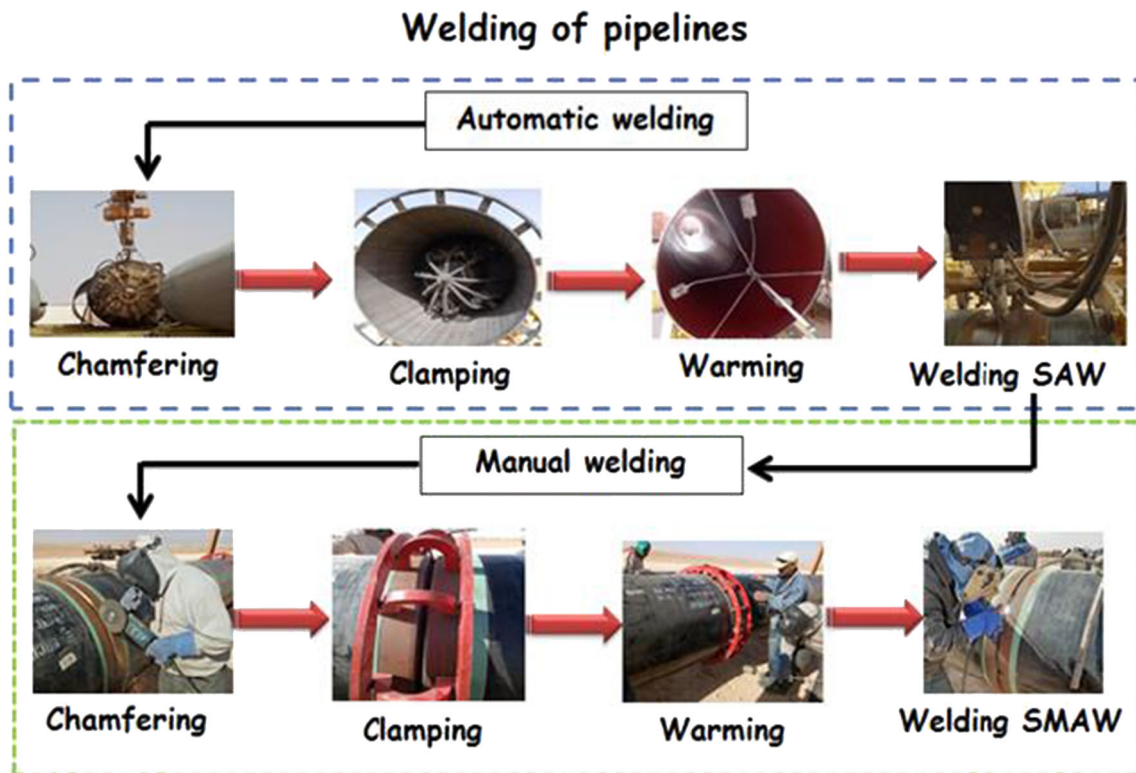


Fig. 2 Process of assembling pipelines

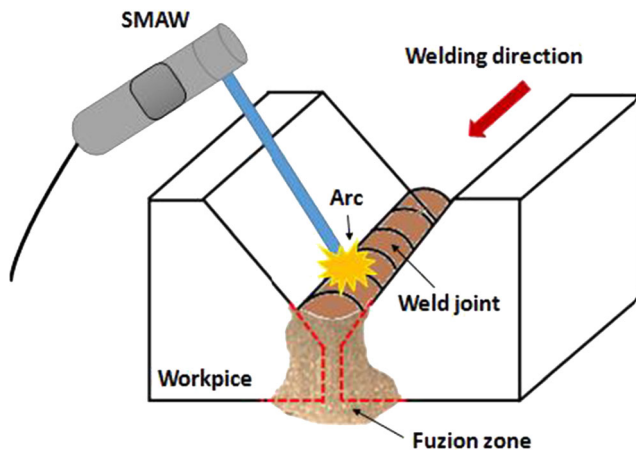


Fig. 3 Principle of the SMAW welding process in V- configuration chamfer

on the one hand and the various interactions between these same parameters on the other hand [9–12]. It is therefore important to better understand the behavior of the SMAW welding process, in order to better master it. The implementation of the experimental designs method makes it possible to highlight the most influential parameters and their interactions on the observables, which are the geometric characteristics of the weld beads.

The synthesis of the results found in the literature allowed a deeper understanding of the behaviors during the assemblies by SMAW welding processes. Patil. Kadam et al [13] have optimized, using the Taguchi method and methodology of response surfaces, the effect of SMAW welding parameters (welding current, welding speed, electrode angle, and root gap) on objective functions (weld strength, metal deposition rate, and bead height are welding current). A.A. Shukla et al [14] analyzed the effect of SMAW welding parameters (welding current, electrode polarity, and torch angle) to maximize the penetration depth. The response surfaces method is introduced in order to acquire optimal welding conditions. Lenin N. et al [15] adopted the Taguchi method for optimization of manual metal arc (MMA) welding parameters, in order to obtain high weld strength. P.G. Ahire et al [16] developed a genetic algorithm model to find the optimal weld deposition rate and weld strength, in the case of SMAW welding. An optimization of the vibratory welding technique during manual arc welding (SMAW) has been

proposed by P.K. Singh et al [17], in order to improve the mechanical properties of a butt weld joint. The Taguchi analysis technique was applied to optimize the process parameters. The study aims to maximize the breaking strength and hardness of welded joints.

The objective of this study is a better understanding of the SMAW manual arc welding process, to ensure a good quality of welding beads. Given the very high level required for the safety of installations in the oil industry, we analyzed the effects of the operating parameters and their interactions on several geometrical quantities which characterize the shape of the melted zone (height of the material deposit H [mm], width of the lower side weld bead $L1$ [mm], and width in the middle of the weld bead $L2$ [mm]). A mathematical model integrating welding process parameters to the dimensions of the weld bead will be established. The analysis of the response surfaces, will allow the likely interactions between the various parameters to be highlighted and their influences on the weld beads morphology.

2 Pipeline assembly process

The study was carried out on 12.000-mm long pipes, with a diameter of 1219.5 mm and a thickness of 13 mm. The material is a steel type API 5L X70, used by the national company SONATRACH for the hydrocarbons pipeline transportation. In order to assemble the pipes to each other for the completion of a continuous line, two arc welding processes are used: the automatic SAW process and the manual SMAW, in view of their advantages vis-à-vis the productivity and maneuverability. Tube assembly operations mainly involves two phases: the first is to assemble the tubes in half using the SAW process (Fig. 1). It is done at the workshop level, to avoid the movement of heavy automatic welding equipment. The second phase aims to assemble, thanks to the SMAW manual electric arc process, all the sections already assembled beforehand by the SAW process. Unlike the first phase, the second is carried out on site, using more manageable hand-held SMAW welding equipment.

Before each assembly, several preparation stages are necessary to ensure very good quality weld beads (Fig. 2). The first step is the preparation of the surface which is an essential operation for the elimination of possible defects. This operation consists of three parts: chamfering, grinding, and brushing (Fig. 2). Proper preparation of the edges to be welded will never make it possible to eliminate at 100% the causes of appearance of the defects, but will in 100% of cases increase the final quality of the welded assembly. In order to obtain an identical gap between the two edges of the two chamfered tubes, the

Table 1 Operating parameters of SMAW welding

Parameters	Values
Welding speed [$\text{mm}\cdot\text{s}^{-1}$]	10
Intensity [A]	115
Voltage [V]	29.5
Diameter of the electrode [mm]	3.25
Polarity	CC-E

Table 2 Chemical compositions of base metal and electrode (wt%)

Materials	Chemical composition (wt%)										
	C	Ni	Ti	S	P	Cu	Mn	Si	V	Cr	Fe
Base metal	0.07	0.05	0.04	0.003	0.013	0.03	1.58	0.29	0.06	0.05	Bal
electrode	0.13	0.07	0.013	0.010	0.006	0.04	0.43	0.20	0.007	0.05	Bal

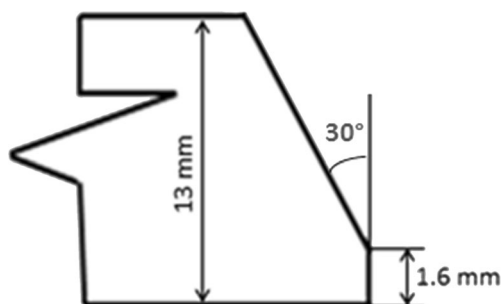
ensuing step of clamping is carried out. The correct execution of this step makes it possible to avoid defects related to the first pass, like the excess of penetration. The last step before welding the tubes is preheating around the welded area. Preheating the steel before starting to weld it, by a propane burner, slows down the cooling of the area to be welded. Preheating will hence reduce the constraints and therefore the development and propagation of cracks in the melted zone (ZF) and especially in the thermally affected zone (ZAT). The need for preheating is proportional to the thickness to be welded, to the constraints related to the carbon content, and the diffusible hydrogen content of the welded metal. Preheating is carried out using gas lances (Fig. 2) or electric heating elements, until a temperature of 100 °C is reached.

3 Description of the process implemented

The purpose of this welding operation is to complete the first pass of the chamfer in v- (Fig.3). This phase is called the heel phase, because it is the most important, as it makes it possible to have a first connection between the two tubes.

3.1 Welding parameters

The operating parameters of the welding were defined at the COSIDER company level. This choice of parameters is linked, on the one hand, to the geometry of the chamfer (it is necessary to avoid the problems of lack of connection bonds and to obtain a good weld bead), and on the other hand, to the material means available to the company (the voltage and

**Fig. 4** Dimensions of the chamfer

intensity of the welding station). The welding parameters used in this case are grouped together in Table 1.

3.2 Pieces to be welded and assembly

For this operation, we use two pieces of X 70 steel whose chemical composition is presented in (Table 2). For the filler metal, we used an E6010 type electrode whose chemical composition is presented in (Table 2), the dimensions of the chamfer, are shown in Fig. 4. A general description of the SMAW welding operation is shown in Fig. 5.

4 Experimental plans approach

The study of a phenomenon or a process supposes the analysis of the evolution of a quantity as a function of the variation of various parameters. In a mathematical form, we can write that the quantity of interest called “objective function,” is a function of several variables called “influence factors.” The modern method (Box-Wilson) is defined by the principle of “all factors in every moment” and uses a multi-factorial strategy.

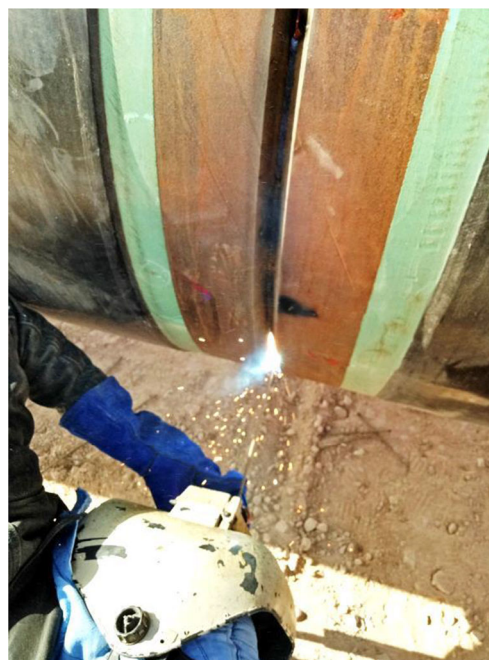
**Fig. 5** General description of the SMAW welding operation

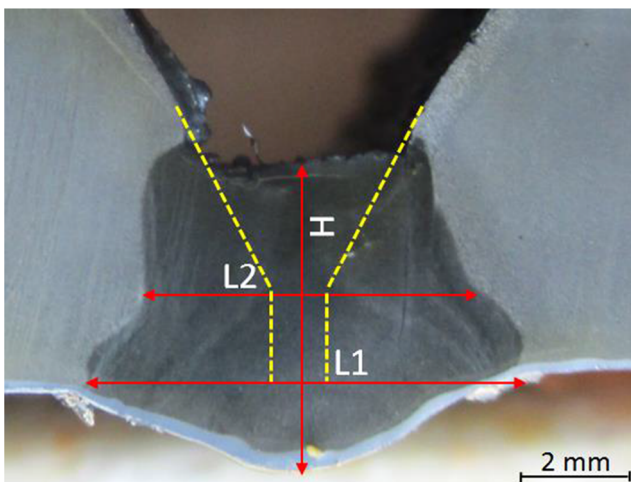
Table 3 Influence factors and their variation domains

Influence factors (IF)	Variation domains
Welding speed V_s [$\text{mm}\cdot\text{s}^{-1}$]	[5; 15]
Voltage T [V]	[26; 32]
Intensity I [A]	[80; 120]
Diameter of the electrode D [mm]	[3.2; 4]

This assumes that levels of all factors be varied at once, but in a planned and rational way. The fact that all factors are varied at once has many advantages [18]. The choice of objective functions has been made taking into account that the pipe welding process is mainly characterized by its productivity and by the quality of the weld beads obtained. The objective functions chosen for this study are the height of the material deposit H [mm], width of the lower side weld bead $L1$ [mm], and the width in the middle of the weld bead (lateral penetration) $L2$ [mm]. We conducted a comprehensive study of these three objective functions. In addition, this study allows us to analyze all the effects of the interactions between the welding process parameters. The objective of this experimental design is to highlight the influence of the following 4 factors: welding speed– V_s [$\text{mm}\cdot\text{s}^{-1}$], voltage– T [V], intensity– I [A], and electrode diameter– D [mm] on the three functions H [mm], $L1$ [mm], $L2$ [mm] so as to provide polynomial empirical models.

The experimental study was conducted using a complete experimental design $\text{CED } 2^4$ (complete factorial design with 4 factors and 2 levels). The experimental model associated with this plan is called linear or first-degree model explained by a polynomial of the form:

$$y = b_0 + \sum_{j=1}^4 b_j x_j + \sum_{\substack{i,j=1 \\ i \neq j}}^4 b_{ij} x_i x_j \quad (1)$$

**Fig. 6** Presentation of the objectives functions (H , $L1$, $L2$).

where y – corresponding objective function

x_j, x_i codified values of influencing factors (± 1).
 b_0, b_j regression coefficients (linear terms).
 b_{ij} regression coefficients (interaction terms).

4.1 Influencing factors (IF)

Among many factors that have a direct or indirect influence on the shape of the melted zone, we have chosen to retain the following operating parameters: the welding speed V_s [$\text{mm}\cdot\text{s}^{-1}$], the voltage of the current T [V], current intensity I [A], and the diameter of the electrode D [mm]. This choice was made based on previous experiences within the national company COSIDER in charge of pipelines on behalf of the national company SONATRACH. We assigned 2 levels to each of the 4 parameters (Table 3). The choice of these levels was defined thanks to the expertise acquired by COSIDER in the field of pipe welding.

4.2 Objective function (OF)

The choice of objective functions (OF) has been established taking into account the fact that the welding of the pipes has been achieved thanks to the SMAW process in the narrow chamfer configuration, is mainly characterized by its productivity in terms of material deposits and by the requirements from an industrial point of view (quality of the beads, strength of the assemblies, etc.). In that case, in order to study the influence of the parameters of the SMAW process on the productivity and the quality of the beads, we have chosen the following objective functions: the height of the material deposit H [mm] corresponding to the productivity, the width of the lower side weld bead $L1$ [mm], and the width of the weld bead in the middle $L2$ [mm] which characterizes the lateral penetration, which is a very important size from an industrial point of view. Figure 6 shows the three objective functions studied as well as the original chamfer.

4.3 Experimental matrix

The experimental matrix for the experimental conditions (04 influential factors with 2 levels and 03 objective functions) includes 16 tests (2^4 trials). The codified and physical levels of the influential factors as well as the measured values of the objective functions (H [mm], $L1$ [mm], and $L2$ [mm]) are presented in Table 4. The experimental tests were performed by a highly qualified welder (certified) and in a random order.

Table 4 Experimental matrix and measured values of objective functions

Test	Influence factors (IF)								Objective functions (OF)		
	Codified values				Physical values				<i>H</i> [mm]	L1 [mm]	L2 [mm]
	<i>T</i>	<i>I</i>	<i>V</i>	<i>D</i>	<i>T</i> [V]	<i>I</i> [A]	<i>V_s</i> [mm.s ⁻¹]	<i>D</i> [mm]			
1	-1	-1	-1	-1	26	80	5	3.2	5.61	7.96	6.37
2	+1	-1	-1	-1	32	80	5	3.2	5.62	8.34	6.29
3	-1	+1	-1	-1	26	120	5	3.2	5.49	8.14	6.59
4	+1	+1	-1	-1	32	120	5	3.2	5.87	10.15	7.47
5	-1	-1	+1	-1	26	80	15	3.2	3.84	7.50	5.67
6	+1	-1	+1	-1	32	80	15	3.2	4.18	7.61	5.57
7	-1	+1	+1	-1	26	120	15	3.2	1.83	5.93	5.12
8	+1	+1	+1	-1	32	120	15	3.2	4.35	10.25	6.46
9	-1	-1	-1	+1	26	80	5	4	5.24	5.03	4.19
10	+1	-1	-1	+1	32	80	5	4	5.69	5.82	5.43
11	-1	+1	-1	+1	26	120	5	4	4.50	5.99	5.59
12	+1	+1	-1	+1	32	120	5	4	4.99	4.63	4.61
13	-1	-1	+1	+1	26	80	15	4	4.58	3.35	2.95
14	+1	-1	+1	+1	32	80	15	4	4.61	5.98	4.39
15	-1	+1	+1	+1	26	120	15	4	6.00	6.85	5.60
16	+1	+1	+1	+1	32	120	15	4	4.97	8.10	6.28

Bold entries is to differentiate between objective functions and influence factors

5 Results and analysis

5.1 Analysis of macrographs

The macrographs are the first information allowing us to find out about the shape and size of the melted zone. They allow us, on the one hand, to validate the numerical models, and on the other hand to study the quality of the weld bead (blowholes, cracks, bonding, etc.). With the operating parameters chosen, penetration is total. Figure 7 shows a wide variety of results concerning the morphology of the weld bead. On the whole of the tests carried out and taking into account the variation domains, the whole set of weld beads show good quality (no bonding and sufficient penetration). Nonetheless, in our case, the morphology of the melted zone obtained is different in contrast to the morphology of the melted zone resulting from other welding processes [10, 19–23]. Usually one finds a wider shape on the upper side with a nail head shape [24]. This is probably related to the hydrodynamic motions of the molten metal. In our case, however, this form is reversed, which is probably related to multiphase phenomena as well as the spreading of energy due to the electric arc on a small thickness of the heel.

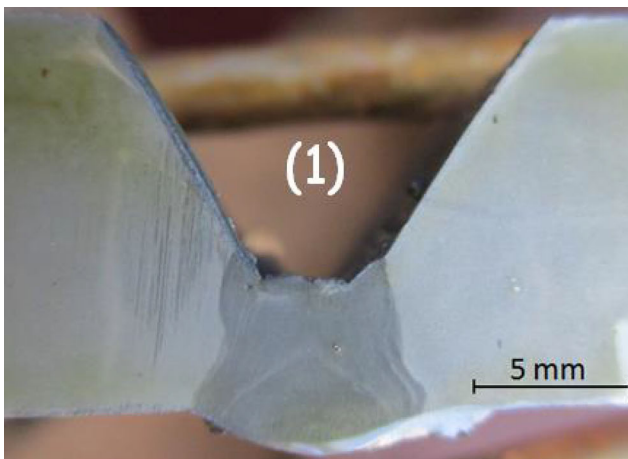
5.2 Analysis of the influence of factors on objective functions

The results of the effects are presented as histograms of PARETO. Figures 8, 9, and 10 represent the effects caused by the influence factors and their interactions on the objective

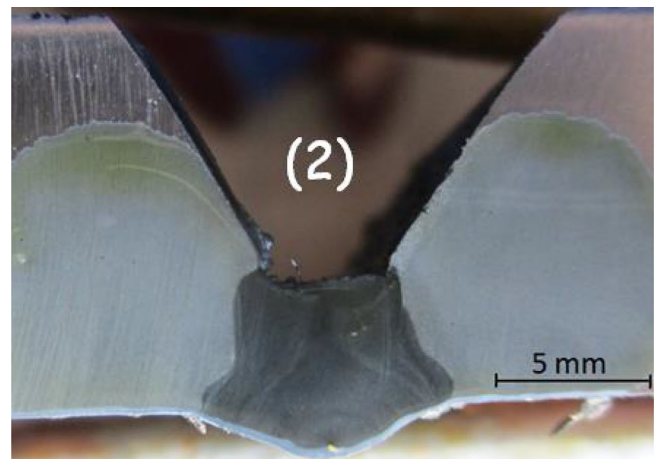
functions studied. We observe in Fig. 8, that the function *H* (height of the deposit) is mainly influenced by the welding speed (*V_s*) and an interaction between the speed and the diameter of the electrode (*D*), followed by the diameter of the electrode. If the speed varies from 5 to 15 mm.s⁻¹, the material deposits height *H* decreases on average by 1.081 mm. By contrast, if the diameter *D* varies from 3.2 to 4 mm, the deposit *H* increases on average by 0.473 mm. Virtually all the work that deals with the study of the effects of welding process parameters on the shape of the weld bead, show that the advance speed is the most influential parameter among the rest of the parameters [23, 25].

In the case of L1 (the width of the lower side weld bead), it is observed that increasing the diameter of the wire *D* generates a decrease in the width of the molten zone lower side. Looking at the hierarchies of the influencing factors (Fig. 9), it is observed that the most influential factor is the diameter of the electrode *D* [mm], followed by the parameters of the energy, the voltage *T*, and the intensity *I*. Complex interactions between *V_s* and the other influencing factors (mainly voltage, electrode diameter, and intensity) also have significant influences on L1. We note that the effect of the speed (*V_s*) on L1 is not significant (very low). On the other hand, it is observed that the indirect effects due to the interactions between speed and *T*, *D*, and *I* are rather significant.

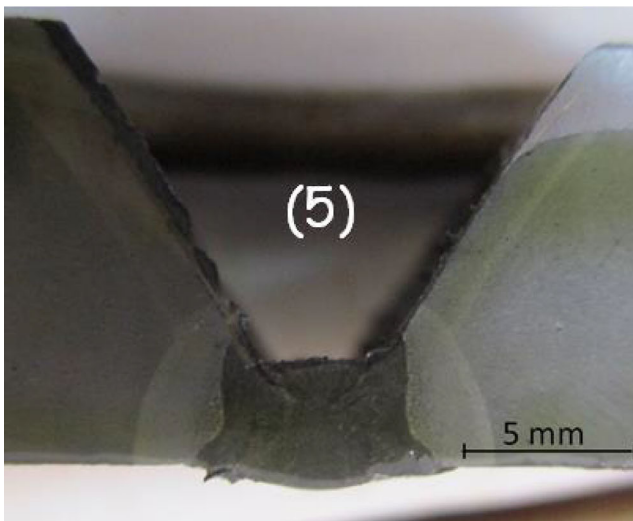
As regards the width in the middle of the weld bead (lateral penetration) L2 [mm], it is, once again, observed that the most influential factor is the diameter of the electrode *D* (Fig. 10), followed this time by the intensity *I*, the speed of advance *V_s*, and the tension *T*.



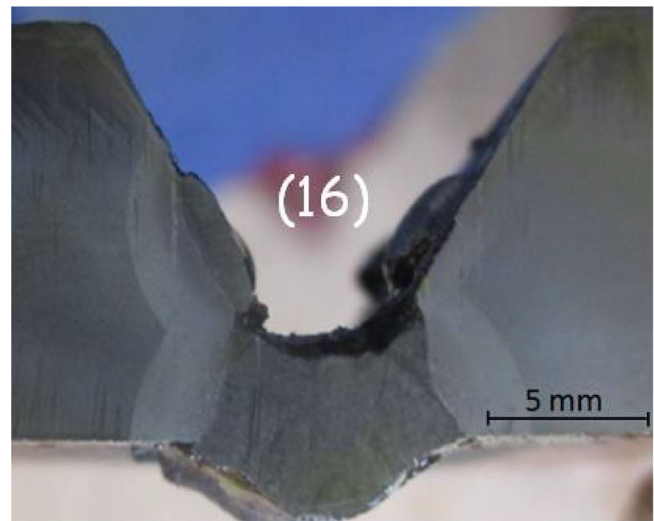
$T= 26V$; $I= 80A$; $V= 5 \text{ mm.s}^{-1}$; $D=3.2\text{mm}$;
 $H= 5.61\text{mm}$; $L1= 7.96 \text{ mm}$; $L2=6.37\text{mm}$



$T= 32V$; $I= 80A$; $V= 5 \text{ mm.s}^{-1}$; $D=3.2 \text{ mm}$;
 $H= 5.62\text{mm}$; $L1= 8.34 \text{ mm}$; $L2=6.29\text{mm}$



$T= 26V$; $I= 80A$; $V= 15 \text{ mm.s}^{-1}$; $D= 3.2 \text{ mm}$;
 $H= 3.84\text{mm}$; $L1= 7.50\text{mm}$; $L2=5.67\text{mm}$



$T= 32V$; $I= 120A$; $V= 15 \text{ mm.s}^{-1}$; $D= 4 \text{ mm}$;
 $H= 4.97 \text{ mm}$; $L1= 8.10\text{mm}$; $L2=6.28\text{mm}$

Fig. 7 Diversity of results and morphologies obtained.

5.3 Analysis of response surfaces

The variation of the material deposits height H as a function of the significant influence factors can be observed in Figs. 11 and 12. Several noteworthy interactions between the influencing factors can be highlighted, on the height H of the weld beads (Figs. 11 and 12). At first, one notices a clear interaction between the welding speed V_s and the electrode diameter D in that, depending on the diameter of the chosen electrode, the effect of the welding speed changes. To illustrate this, for a diameter $D = 3.2 \text{ mm}$, an increase of the speed V_s causes a sharp decrease in the height H . However, in the case of a diameter $D = 4 \text{ mm}$, the variation of the velocity hardly affects

the height of the deposit H . Moreover, it is noticed that there is an interaction between the tension T and the electrode diameter D in that for a diameter $D = 3.2 \text{ mm}$, the increase of the tension T causes a significant increase in the height H . However, in the case of a diameter $D = 4 \text{ mm}$, the variation of the tension T has very little influence on the height H .

The response surface analysis for the size L1 shows that, for an electrode diameter $D = 3.2 \text{ mm}$, the welding speed V_s has little influence on L1. On the other hand, for a diameter of $D = 4 \text{ mm}$, the increase in welding speed entails an increase in L1; consequently, we have an interaction between D and V_s (Fig. 13). Furthermore, we observe the presence of a strong interaction between V_s and T , in the sense that the T levels

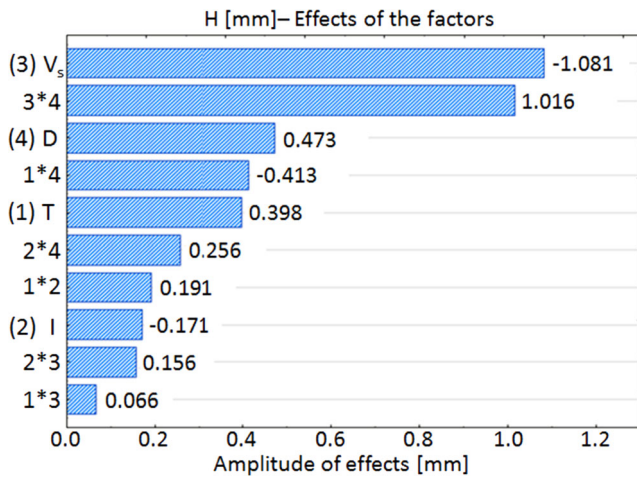


Fig. 8 Influence of the factors on the height of the deposit H [mm]

influence the effect of V_s on L1: for $T = 26$ V a decrease of L1 is observed with the increase of V_s , whereas for $T = 32$ V the effect of V_s on L1 is opposite, thus L1 increases with the increase of V_s (Fig.14).

With regard to the size L2, a certain interaction between the electrode diameter D and the current intensity I can be demonstrated (Fig. 15): for a value $I = 80$ A, there is a sharp increase in L2 with the decrease in the electrode diameter D . On the other hand, this increase of L2 is much less important with the decrease of D , for a value of $I = 120$ A.

Finally, a rather weak interaction is also present between D and V_s (Fig.16), with regard to L2: for a feed rate $V_s = 5$ mm.s⁻¹, L2 increases significantly with a decrease in D , but this increase is less important for a speed $V_s = 15$ mm.s⁻¹.

5.4 Development of the experimental model

From the histograms of PARETO (Figs.8, 9, and 10) and the coefficients of the influence factors, we can write the law of

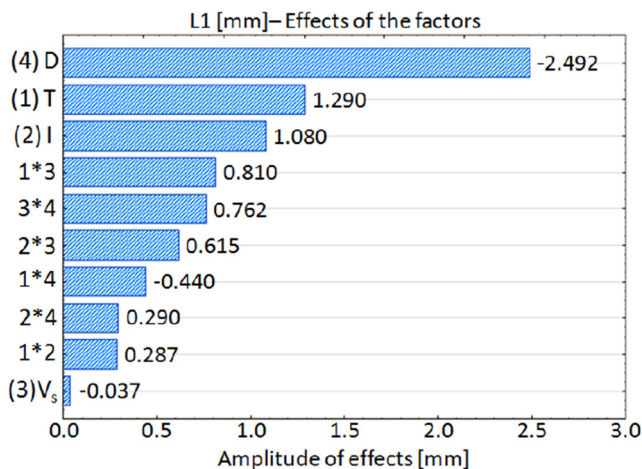


Fig. 9 Influence of the factors on the width of the lower side weld bead L1 [mm]

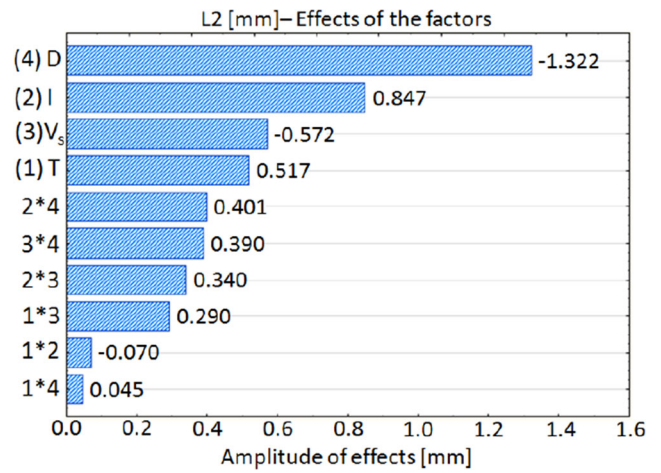


Fig. 10 Influence of the factors on the width at the middle of the weld bead L2 [mm]

variation of the three objective functions (height of the deposit H [mm], the width of the lower side weld bead L1 [mm], the width at the middle of the weld bead L2 [mm]) as a function of the welding operating parameters, and their interactions (T , I , V_s and D).

$$H = 4.835 - 0.540 V_s + 0.508 V_s D - 0.236 D - 0.206 T D + 0.199 T \quad (2)$$

$$L1 = 6.976 - 1.246 D + 0.645 T + 0.54 I + 0.405 T V_s + 0.381 V_s D + 0.307 I V_s \quad (3)$$

$$L2 = 5.525 - 0.666 D + 0.423 I - 0.286 V_s + 0.258 T + 0.2 I D \quad (4)$$

To validate the experimental model, we have compared the values of the three estimated objective functions (H , L1, and L2) to the model whose values are measured on the

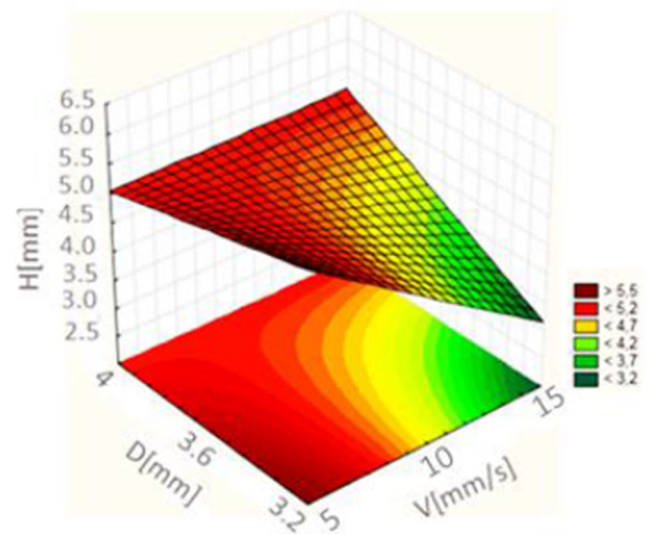


Fig. 11 Variation of the height of the weld bead H with V_s and D

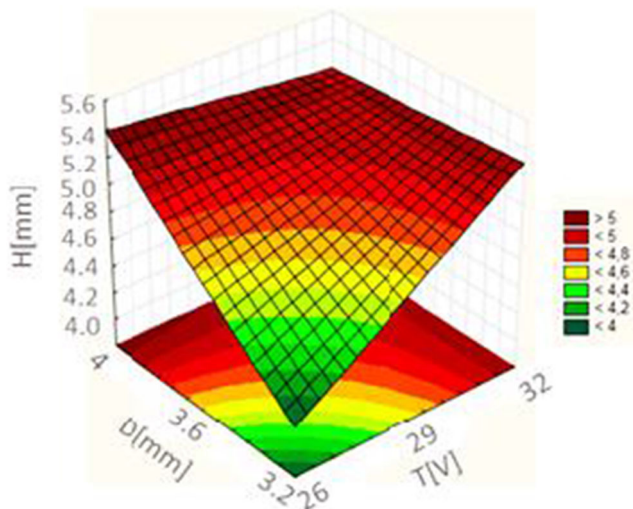


Fig. 12 Variation of the height of the weld bead H with T and D

macrographs. We find a good agreement between the measurements and the estimated values (Figs.17, 18, and 19).

6 Conclusion

Despite the development of new welding technologies, the SMAW manual electric arc process remains essential in pipeline assembly operations. This welding technique offers several advantages such as: good productivity, welding in all positions, low costs, and good quality beads. In order to master the SMAW welding process, the experimental approach using the experimental designs method allowed us to highlight the following results:

- (1) The morphology of the melted zone obtained (case of filling narrow chamfers by SMAW welding) is different compared to other shapes from other welding processes.

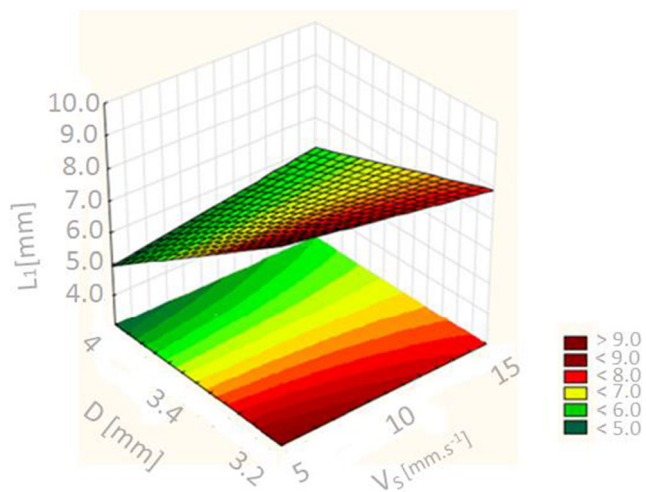


Fig. 13 Variation in the width of the lower side weld bead $L1$ with D and V_s

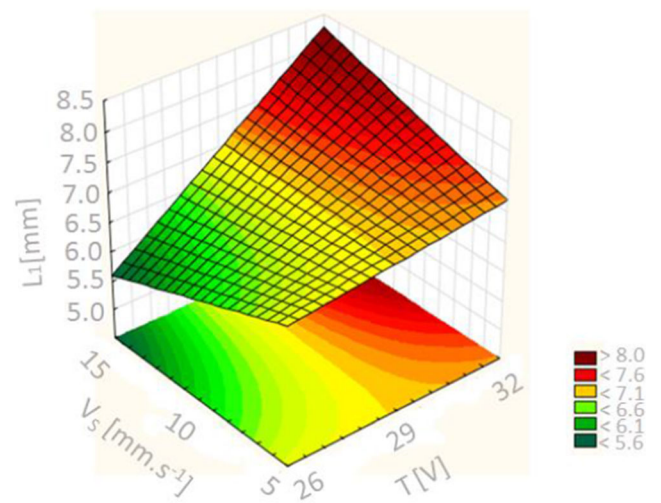


Fig. 14 Variation in the width of the lower side weld bead $L1$ with V_s and T

- Usually we find the shape of a nail head on the upper side of the weld bead. On the other hand, in the case of SMAW welding, the shapes are reversed, which is probably related to multi-physical phenomena and the spreading of energy on a small thickness due to the electric arc.
- (2) The material deposits height H is mainly influenced by the welding speed and an interaction between the welding speed and the diameter of the electrode. The width of the melted zone lower side $L1$ and the width in the middle of the melted zone (lateral penetration) $L2$ are influenced mainly by the diameter of the electrode.
- (3) The effect of the welding speed on the width of the lower side weld bead $L1$ is not significant (very low) contrary to the material deposits height H . On the other hand, one observes that the interaction between the welding speed V_s and the other three parameters (the voltage T , the

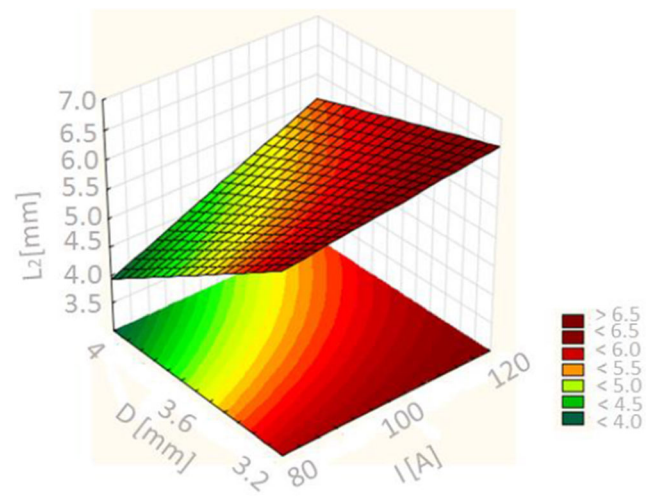


Fig. 15 Variation of the width in the middle of the weld bead $L2$ with D and I

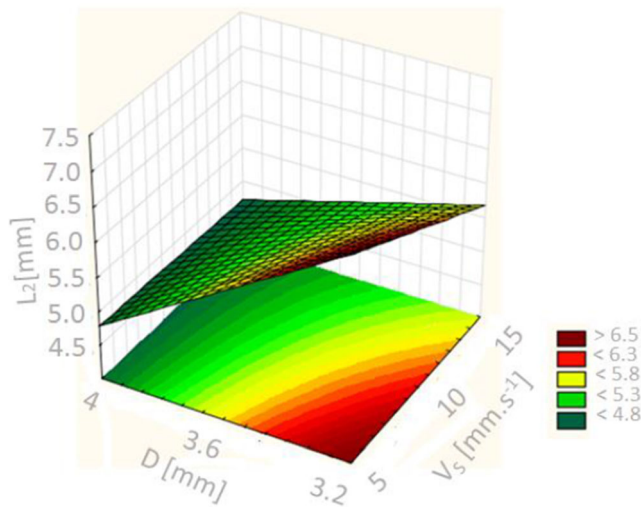


Fig. 16 Variation of the width in the middle of the weld bead L_2 with D and V_s

electrode diameter D , and the current intensity I) are significant.

- (4) Depending on the diameter of the chosen electrode, the effect of the welding speed V_s on the height of material deposits H is different. For a diameter of 3.2 mm, one notices a sharp decrease in the height H with the increase in the speed V_s . On the other hand, for a diameter of 4 mm, speed variation does not have any influence over H .
- (5) The effect of the tension T over H varies, in that, for a 3.2-mm diameter, a sharp increase in H is observed when the tension is increased. In contrast, for a diameter of 4 mm, variation in the tension does not virtually have any effect on H .
- (6) For a 3.2-mm diameter electrode, the welding speed has little influence over the width of the lower side weld bead L_1 , whereas, for a 4-mm diameter, an increase in the speed involves an increase in L_1 . Moreover, a strong

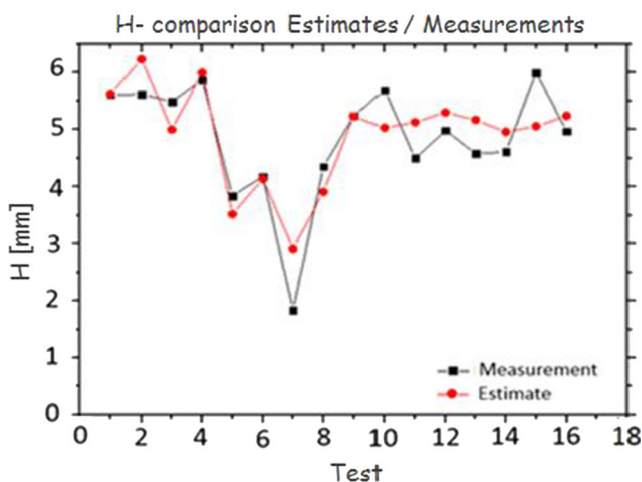


Fig. 17 Comparison between measurements and estimated values of height deposit (H)

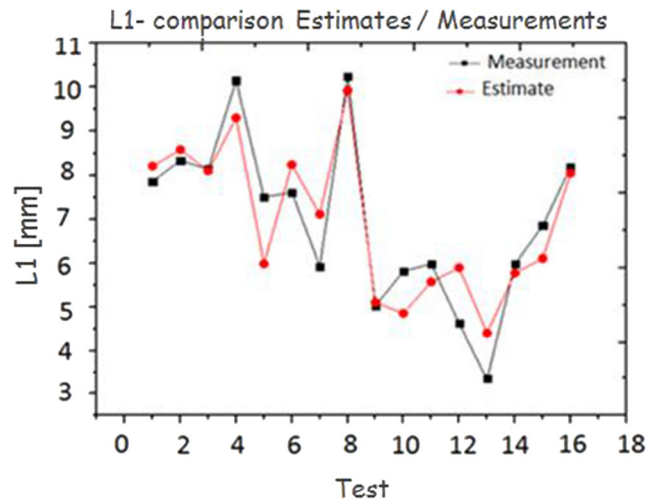


Fig. 18 Comparison between measurements and estimated values of width of the weld bead (L_1)

interaction is noticed between the speed and the tension, such that, various levels of the tension T influence the way V_s affects L_1 .

- (7) For a value of the current intensity equal to 80A, one notices a sharp increase in the lateral penetration L_2 , with a decrease in the electrode diameter D . By contrast, this increase in L_2 is much less significant with a decrease in D , for a current intensity equal to 120 A.
- (8) The experimental results obtained as part of this work can contribute on the one hand for the validation of numerical models. On the other hand, they can help understand the phenomena which intervene during welding operations in order to take them into consideration when developing numerical models.

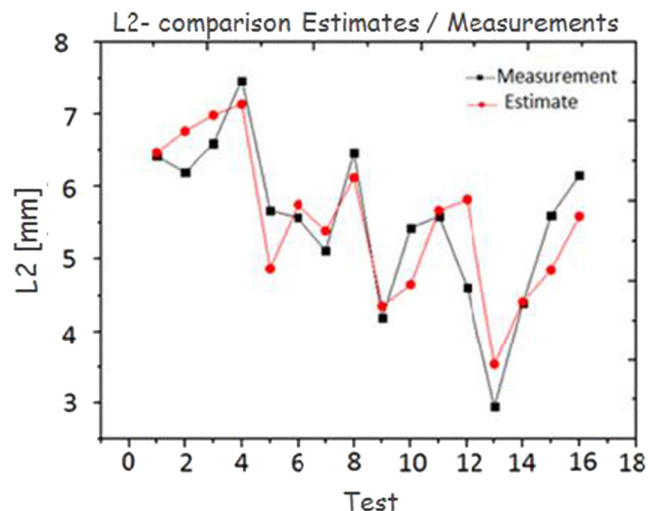


Fig. 19 Comparison between measurements and estimated values of lateral penetration (L_2)

References

- Sidhu GS, Chatha SS (2012) Role of shielded metal arc welding consumables on pipe weld joint. *Int J Emerg Technol Adv Eng* 2(12):ISSN 2250-2459
- Mvola B, Kah P, Martikainen J, Suoranta R (2014) State-of-the-art of advanced gas metal arc welding processes: Dissimilar metal welding. *Proc Inst Mech Eng B J Eng Manuf* 229:1694–1710
- Anren Y, Zhen L, Sansan A (2012) A CMOS Visual Sensing System for Welding Control and Information Acquirement in SMAW Process. *Phys Procedia* 25:22–29
- Selvi S, Sankaran SP, Srivatsavan R (2008) Comparative study of hardfacing of valve seat ring using MMAW process. *J Mater Process Technol* 207:356–362
- Saxena A, Kumaraswamy A, Madhusudhan Reddy G, Madhu V (2018) Influence of welding consumables on tensile and impact properties of multi-pass SMAW ArmoX 500 T steel joints vis-a-vis base metal. *Defence Technol* 14:188–195
- Jorge LDJ, Cândido VS, Silva ACRD, Filho FDCG, Pereira AC, Luz FSD, Monteiro SN (2018) Mechanical properties and microstructure of SMAW welded and thermally treated HSLA-80 steel. *J Mater Res Technol* 7:598–605
- Raffi M, Madhusudhan Reddy G, Srinivasa Rao K (2015) Microstructure and pitting corrosion of shielded metal arc welded high nitrogen stainless steel. *Defence Technol* 11:237–243
- Verma J, Taiwade RV, Khatirkar RK, Sapate SG, Gaikwad AD (2016) Microstructure, Mechanical and Intergranular Corrosion Behavior of Dissimilar DSS 2205 and ASS 316 L Shielded Metal Arc Welds. *Trans Indian Inst Metals* 70:225–237
- Dhas J, Sathesh M (2013) Sensitivity analysis of submerged arc welding parameters for low alloy steel weldment. *Indian J Eng Mater Sci* 20:425–434
- Singh RP, Garg R, Shukla DK (2016) Mathematical modeling of effect of polarity on weld bead geometry in submerged arc welding. *J Manuf Process* 21:14–22
- Hayajneh MT, Al-Dwairi AF, Obeidat SF (2018) Optimization and control of bending distortion of submerged arc welding I-beams. *J Constr Steel Res* 142:78–85
- Sailender M, Reddy GC, Venkatesh S (2018) Influences of process parameters on weld strength of low carbon alloy steel in purged SAW. *Materials Today: Proceedings* 5:2928–2937
- Patil US, Kadam MS (2020) Multiobjective optimization of MMAW process parameters for joining stainless steel 304 with mild steel by using response surface methodology. *Materials Today: Proceedings* 26:305–310
- Shukla AA, Joshi VS, Chel A, Shukla BA (2018) Analysis of Shielded metal arc welding parameter on Depth of Penetration on AISI 1020 plates using Response surface methodology. *Procedia Manuf* 20:239–246
- Lenin N, Sivakumar M, Vigneshkumar D (2010) Process parameter optimization in ARC welding of dissimilar metals, Thammasat. *Int J Sc Tech* 15(3)
- Ahire PG, Patil US, Kadam MS (2018) Genetic algorithm based optimization of the process parameters for manual metal arc welding of dissimilar metal joint. *Procedia Manuf* 20:106–112
- Singh PK, Patel D, Prasad S (2016) Optimization of process parameters during vibratory welding technique using Taguchi's analysis. *Perspect Sci* 8:399–402
- Goupy J (2001) *Introduction aux plans d'expériences*, 2nd edn. Dunond, Paris
- Huang H-Y (2010) Effects of activating flux on the welded joint characteristics in gas metal arc welding. *Materials & Design* (1980-2015) 31:2488–2495
- Martinez-Conesa EJ, Egea JA, Miguel V, Toledo C, Meseguer-Valdenebro JL (2017) Optimization of geometric parameters in a welded joint through response surface methodology. *Constr Build Mater* 154:105–114
- Srivastava S, Garg R (2017) Process parameter optimization of gas metal arc welding on IS: 2062 mild steel using response surface methodology. *J Manuf Process* 25:296–305
- Bidi L, Mattei S, Cicala E, Andrzejewski H, Le Masson P, Schroeder J (2011) The use of exploratory experimental designs combined with thermal numerical modelling to obtain a predictive tool for hybrid laser/MIG welding and coating processes. *Opt Laser Technol* 43:537–545
- Bidi L, Le Masson P, Cicala E, Primault C (2017) Experimental design method to the weld bead geometry optimization for hybrid laser-MAG welding in a narrow chamfer configuration. *Opt Laser Technol* 89:114–125
- Ahna J, Chenb L, Heb E, Deara JP, Daviesa CM (2018) Optimisation of process parameters and weld shape of high power Yb-fibre laser welded 2024-T3 aluminium alloy. *J Manuf Process* 34:70–85
- Ibrahim IA, Mohamat SA, Amir A, Ghalib A (2012) The Effect of Gas Metal Arc Welding (GMAW) processes on different welding parameters. *Procedia Eng* 41:1502–1506

Publisher's note Springer Nature remains neutral with regard to jurisdictional claims in published maps and institutional affiliations.